Supporting Information

Single-Molecule Analysis of MicroRNA and Logic Operations Using a Smart Plasmonic Nanobiosensor

Ying Zhang,[†] Zhenhua Shuai,[†] Hao Zhou,[†] Zhimin Luo,[†] Bing Liu,[‡] Yinan Zhang,[‡] Lei Zhang,[*,†] Shufen Chen,[†] Jie Chao,[†] Lixing Weng,[†] Quli Fan,[†] Chunhai Fan,[†,‡] Wei Huang,[†,⊥] and Lianhui Wang[*,†]

[†]Key Laboratory for Organic Electronics and Information Displays & Jiangsu Key Laboratory for Biosensors, Institute of Advanced Materials (IAM), Jiangsu National Synergistic Innovation Center for Advanced Materials (SICAM), College of Electronic and Optical Engineering & College of Microelectronic, Nanjing University of Posts & Telecommunications, 9 Wenyuan Road, Nanjing 210023, China

[‡]Division of Physical Biology & Bioimaging Center, Shanghai Synchrotron Radiation Facility, Key Laboratory of Interfacial Physics and Technology, Shanghai Institute of Applied Physics, Chinese Academy of Sciences, Shanghai 201800, China

[⊥]Key Laboratory of Flexible Electronics (KLOFE) and Institute of Advanced Materials (IAM), Jiangsu National Synergistic Innovation Center for Advanced Materials (SICAM), Nanjing Tech University, Nanjing 210028, China

***Corresponding Author**

iamlzhang@njupt.edu.cn

iamlhwang@njupt.edu.cn

This PDF file includes:

Materials and Methods

Chemicals and Materials. Silver nitrate ($AgNO_3$), gold (III) chloride trihydrate ($HAuCl_4 \cdot 3H_2O$), L-ascorbic acid (AA), sodium borohydride ($NaBH_4$), cetyltrimethylammonium bromide (CTAB), and cetyltrimethy-lammonium chloride (CTAC) were purchased from Sigma-Aldrich, and used as received. Endonucleases *Kpn*I, *Stu*I, *Hind*III and *Sal*I were purchased from Takara Biotechnology Co. Ltd. (Dalian, China). Other chemicals with at least analytical grade were used as received. All the chemicals were used without additional purification. The buffer solutions used in this study are as follows: the tetrahedron-structured DNA (tsDNA) assembly buffer solution was TM buffer solution (20 mM Tris, 50 mM $MgCl_2$, pH 8.0). The buffer solution for hybridization was 1 M NaCl and 10 mM TE buffer solution (pH 7.4). All solutions were prepared with RNase-free water. The RNase-free water was prepared with Milli-Q water (18 MΩ cm) from a Millipore system treated with 0.1% DEPC and stored at 4 °C.

All oligonucleotides were provided by Takara Biotechnology Co. Ltd. (Dalian, China) and the sequences were shown in Table S1.

Synthesis of 30 nm Au Nanocrystal Seeds. A three-step procedure was used for synthesizing the 30 nm Au nanocrystal seeds.[1] 1) Au seeds with the average diameter of 3 nm were prepared by rapidly injecting freshly prepared 0.6 mL of ice cooled $NaBH_4$ solution (10 mM) into a mixture solution composed of $HAuCl_4$ (0.25 mM) and CTAB (100 mM) under vigorous stirring. To ensure complete decomposition of $NaBH_4$ in the solution, the mixture was kept at a constant temperature of 28 ^oC for 3 h. 2) 3 mL of AA aqueous solution (100 mM) was added into 12 mL of aqueous solution containing $HAuCl_4$ (0.25 mM) and CTAC (100 mM) under rapid stirring and then 0.3 mL of the 3 nm Au seeds was added. The color of mixture turned from colorlessness to red and was further kept undisturbed for 1 h at 36 °C to prepare 10 nm Au seeds. 3) 30 nm Au seeds were prepared by adding 1 mL of the 10 nm Au seeds (10 nM) into 19 mL of aqueous solution containing 8 mL of $HAuCl_4$ aqueous solution (0.5 mM), 8 mL of CTAC aqueous solution (200 mM) and 3 mL of AA aqueous solution (100 mM). After stirring for 5 min, the mixture was kept at 36 ^oC for 1 h and used as seed solution for the synthesis of 55 nm Au@Ag Core-Shell Nanocubes (Au@Ag NCs).

Synthesis of 55 nm Au@Ag NCs. In brief, 3 mL of the prepared 30 nm Au seeds was mixed with 7 mL of CTAC aqueous solution (20 mM) in a 20 mL vial, and then 3 mL of AA aqueous solution (100 mM) was added as a reducing agent. The mixture was heated at 60 ^oC and stirred for 20 min, and then 0.6 mL of $AgNO_3$ aqueous solution (10 mM) was simultaneously added at a rate of 0.04 mL/min using a syringe pump until the color of solution turned from red to brownish yellow, and was further kept undisturbed for 3 h at 60 ^oC. After the solution was cooled to room temperature, the products were collected by centrifugation at the speed of 5000 rpm for 10 min and washed with water twice.

Characterization. Absorption spectra of Au@Ag NCs were recorded using a Shimadzu UV3600 spectrometer. Scanning electron microscope (SEM) images were

obtained with a S-4800 microscope operated at 200 kV (Japan). Transmission electron microscope (TEM) images were collected with a JEM 2010 microscope operated at an acceleration voltage of 200 kV (Japan). Structural analysis of the selected Au@Ag NC was performed in scanning TEM (STEM) mode on a Philips CM 200 electron (200 kV) equipped with an energy dispersive X-ray spectrometer (EDS). The STEM image was recorded with a high-angle annular dark-field (HAADF) detector. SEM samples were prepared by dropping the Au@Ag NC colloidal solution on ITO glass substrates and being dried at room temperature. TEM and STEM samples were prepared by dropping the Au@Ag NC colloidal solution on a holey carbon-coated copper grid and then being dried in air. All the measurements were obtained at room temperature.

Formation of tetrahedron-structured DNA. Tetrahedron-structured DNA (tsDNA) was synthesized based on the modified reported method.[2] Tetra-A and three thiol-modified single strands (tetra-B, tetra-C, and tetra-D, the sequences shown in Table S1) were dissolved in the TM buffer solution (20 mM Tris, 50 mM $MgCl_2$, pH 8.0) with equimolar quantities (combinations of tsDNA strands shown in Table S2). The resulting mixture was heated to 95 ℃ for 10 min and then cooled to 4 ^{o}C over 5 min. For DNA assays: The tsDNA was analyzed using polyacryamide gel electrophoresis (PAGE) in the TBE buffer solution (89 mM Tris, 89 mM boric acid, 2 mM EDTA, pH 8.3) at a constant current of 5 mA at 4 ^{o}C.

Preparation of sensing substrate. For our experiments, indium tin oxide (ITO) glass slides were cleaned by rinsing with soapy water, acetone, ethanol and water under ultrasonication for 1 h, respectively, and then dried under nitrogen blowing. The Au@Ag NCs were immobilized on the cleaned ITO glass slide by physical adsorption from diluted solution for 1 min, and then the surface of ITO glass slides was rinsed with water and dried under a stream of nitrogen.

Modification of tetrahedron-structured DNA (tsDNA) on the surface of Au@Ag NC. In order to combine Au@Ag NC sufficiently, tsDNA was designed to have a thiol group at 5' ends of Tetra-B, Tetra-C and Tetra-D, respectively. For preparation of the biosensor surface with tsDNA, the tsDNA solution (concentration, 1 pM) in running buffer was immobilized on the surface of the Au@Ag NCs modified ITO glass. Immobilization was done at room temperature under constant mixing in the shaker for 3 h. Then, the ITO glass were rinsed with water and dried in a weak stream of nitrogen. The tsDNA molecules were anchored on the surface of Au@Ag NC via specific Au-S bonding according to the previous report.[3]

tsDNA-miRNA hybridization reaction. In a typical hybridization experiment, 200 μL of miR-21 solution in aforementioned hybridization buffer solution, 50 % fetal bovine serum (FBS) or human serum (HS) was dropped onto the surface of aforementioned Au@Ag NC-tsDNA modified ITO glass slides. The hybridization reaction was carried out at room temperature for 3 h, and then the surface of ITO glass slides was rinsed with RNase-free water and dried in a weak stream of nitrogen.

Cleavage reaction of $tsDNA_{17}$ on Au@Ag NC-$tsDNA_{17}$ probes or Au@Ag NC-$tsDNA_{17}$-miR-21 nanoconjugates. Test digestions of DNA with endonucleases *Kpn*I and *Stu*I were performed according to the manufacturer's instructions from

Takara Biotechnology Co. Ltd. (Dalian, China). The cleavage sites for the two endonucleases are shown in Table S1. 1 μL of each of the endonucleases were mixed along with appropriate amounts of buffer and water in 50 μL final reaction volume. For cleavage reaction of $tsDNA_{17}$ on Au@Ag NC-$tsDNA_{17}$ probes or Au@Ag NC-$tsDNA_{17}$-miR-21 nanoconjugates, 100 μL of the aforementioned endonuclease mixture were pipetted onto the surface of the functionalized ITO glass slides. The reaction was incubated at 37 ^{o}C in a shaker for 15 min. The digestion was then verified by 8% PAGE in 1X TBE, with a 20 bp ladder as a molecular weight standard provided from Takara Biotechnology Co. Ltd. (Dalian, China) (Figure S9).

Single-particle DFM imaging and scattering spectroscopy. An inverted microscope (eclipse Ti-U, Nikon, Japan) equipped with a dark-field condenser ($0.8 < NA < 0.95$), a 100 W halogen lamp, a monochromator (Acton SP2300i) equipped with a spectrograph CCD (PIXIS 400BR: excelon, Princeton Instruments), and a true-color digital camera (Nikon DS-fi2) and a grating (grating density: 300 L/mm; blazed wavelength: 500 nm) were used for the dark-field spectrum measurements. The true-color scattering images of Au@Ag NCs were taken using a 60X objective lens. The scattering spectra from the individual Au@Ag NC were corrected by subtracting the background spectra taken from the adjacent regions without the Au@Ag NC and dividing with the calibrated response curve of the entire optical system. The Au@Ag NC-functionalized ITO glass slides were placed on the platform. At first, the scattering light of a single tsDNA-modified Au@Ag NC was set as the initial spectral wavelength. Secondly, 200 μL of miR-21 solution was added to the surface of ITO glass slide. The time-dependent scattering spectra of the single tsDNA-modified Au@Ag NC were obtained to monitor the hybridization process in real time with the final concentration of 1 pM miR-21 (Figure S5). In order to study the cleavage reaction of $tsDNA_{17}$, the endonucleases in buffer solution (100 μL final volume) were dropped onto the functionalized surface of ITO glass slides at 37 ^{o}C for 15 min, and then the spectra were collected by the single-particle DFM imaging and scattering spectroscopy. The spectra were taken with integration time of 20 s.

FDTD simulations. Finite-difference time-domain (FDTD) treats MaxWell equations as a finite differential equation in the scale of both time and space, and the software package FDTD Solutions (version: 8.7.1072, Lumerical Solutions Inc, Vancouver Canada) was used to carry out the FDTD simulations. In the process of computational calculations, the incident light is circularly polarized with the wavelength ranging from 300 to 800 nm and the mesh sizes in the x, y, z directions were all fixed to 0.5 nm. Perfectly matched layer (PML) absorbing boundary were used in all directions. To be consistent with the experiments, the Ag NC shell with a core of Au NP was put onto the glass substrate, and the refractive index (RI) of the surrounding environment (water) was set to be 1.33. All materials used the data from the model of Palik.[4] According to the TEM images and in-situ SEM images (Figure 1c,e), the radius of Au nanosphere was determined to be 15 nm, edge length of the Ag nanocube was about 56 nm. Besides, all corners and edges of the nanocube were rounded with a radius of 9 nm. According to experiments, the single Au@Ag NC plasmonic probe was fabricated by assembly of $tsDNA_{17}$ on the surface of an Au@Ag

NC. A thin film (layer A) with the thickness of 5 nm composed of $tsDNA_{17}$ and H_2O molecules was formed (Figure 2a-I). The refractive index (RI) of layer A was set to be 1.75, which is between the RI of DNA and H_2O molecules.[5] After treatment with miR-21, the miRNAs took the place of H_2O molecules between the DNA arrays near the surface of Au@Ag NCs during the hybridization process and the RI increased. A $tsDNA_{17}$-miR-21 molecule layer (layer B) has the same thickness as layer A, while the RI of layer B was set to be 1.90, which represents the completely ligand (Figure 2a-II). Since the remaining miR-21 molecule layer with the thickness of 4 nm outside the tetrahedral structure (layer C) consisted of single strand nucleic acid molecules, the RI of layer C was set to be 1.70 (Figure 2a-II). The thicknesses of the layer A, layer B and layer C were selected based on the used $tsDNA_{17}$ and $tsDNA_{17}$-miR-21 in experiments. By setting the RI of layer A, layer B and layer C to be 1.75, 1.90 and 1.70, respectively, the simulated LSPR scattering spectra of the single Au@Ag NC-$tsDNA_{17}$ and Au@Ag NC-$tsDNA_{17}$-miR-21 were found to be consistent with the LSPR scattering spectra observed in the experiments after $tsDNA_{17}$ and miR-21 hybridization (Figure 2b,c). The values of 1.75, 1.90 and 1.70 are reasonable since they both lie in the range from 1.33 to 1.96, where 1.33 is the RI of H_2O molecules and 1.96 is the RI of DNA.[6]

Table S1 The sequences of oligonucleotides (from 5′to 3′end) used in this work.

oligonucleotide	Sequence (5-3)*
Tetra-A_7	GAGCGTTAGCCACACACACAGTCTCAACATCAGT
Tetra-B_7	HS-C6-TTAGGCGAGTGTGGCAGAGGTGT
Tetra-C_7	HS-C6-CGCCTAAACAAGTGGAGACTGTG
Tetra-D_7	HS-C6-AACGCTCACCACTTGAACACCTC
Tetra-A_{17}	TCTGAAACATTACAGCTTGCTACACGAGACGGGGTACCCCGGTA
Tetra-B_{17}	HS-C6-TATCACCAGGCAGTTGACAGTGTAGCAAGCTGTAATAGATGCGAGGGTCCAATAC
Tetra-C_{17}	HS-C6-TCAACTGCCTGGTGATAAAAAGGCCTTACGTGGGAATCTACCGGGGTACCCCGTC
Tetra-D_{17}	HS-C6-TTCAGATCAACATCAGTGCTTCCCACGTAAGGCCTTTTGTATTGGACCCTCGCAT
Tetra-A_{26}	GCCTGGAGATACATGTTTCGCGCACCTGAGACCTTCTAATAGGGTTTGCGACAGTCGTTCAACTAGAATGCCC
Tetra-B_{26}	HS-C6-GGGCTGTTCCGGGTGTGGCTCGTCGGTTTCCCTATTAGAAGGTCTCAGGTGCGCGTTTCGGTAAGTAGACGGGACCAGTTCGCC
Tetra-C_{26}	HS-C6-CCGACGAGCCACACCCGGAACAGCCCTTTCCGCAGCGGAGCAGGAGTCCTCGGCCTTTGGGCATTCTAGTTGAACGACTGTCGC
Tetra-D_{26}	HS-C6-CATGTATCTCCAGGCTCAACATCAGTTTTTGGCCGAGGACTCCTGCTCCGCTGCGGTTTGGCGAACTGGTCCCGTCTACTTACCG
miR-21	UAGCUUAUCAGACUGAUGUUGA
Single-base mismatch miRNA	UAGCUUAUCAGAC<u>C</u>GAUGUUGA
Random-miRNA	CUGACCUAUGAAUUGACAGCC

* The mutation base is marked out by underline.

Table S2 Construction of tetrahedral nanostructures.

Tetrahedron-structured DNA	Description	DNA strand combination
$tsDNA_7$	miR-21-responsive tsDNA	Tetra-A_7+Tetra-B_7+Tetra-C_7+Tetra-D_7
$tsDNA_{26}$	miR-21-responsive tsDNA	Tetra-A_{26}+Tetra-B_{26}+Tetra-C_{26}+Tetra-D_{26}
$tsDNA_{17}$	miR-21-responsive tsDNA	Tetra-A_{17}+Tetra-B_{17}+Tetra-C_{17}+Tetra-D_{17}
$tsDNA_{17}$	endonucleases-responsive tsDNA	Tetra-A_{17}+Tetra-B_{17}+Tetra-C_{17}+Tetra-D_{17}
$tsDNA_{17}$ for detection in fetal bovine serum		Tetra-A_{17}+Tetra-B_{17}+Tetra-C_{17}+Tetra-D_{17}
$tsDNA_{17}$ for detection in human serum		Tetra-A_{17}+Tetra-B_{17}+Tetra-C_{17}+Tetra-D_{17}

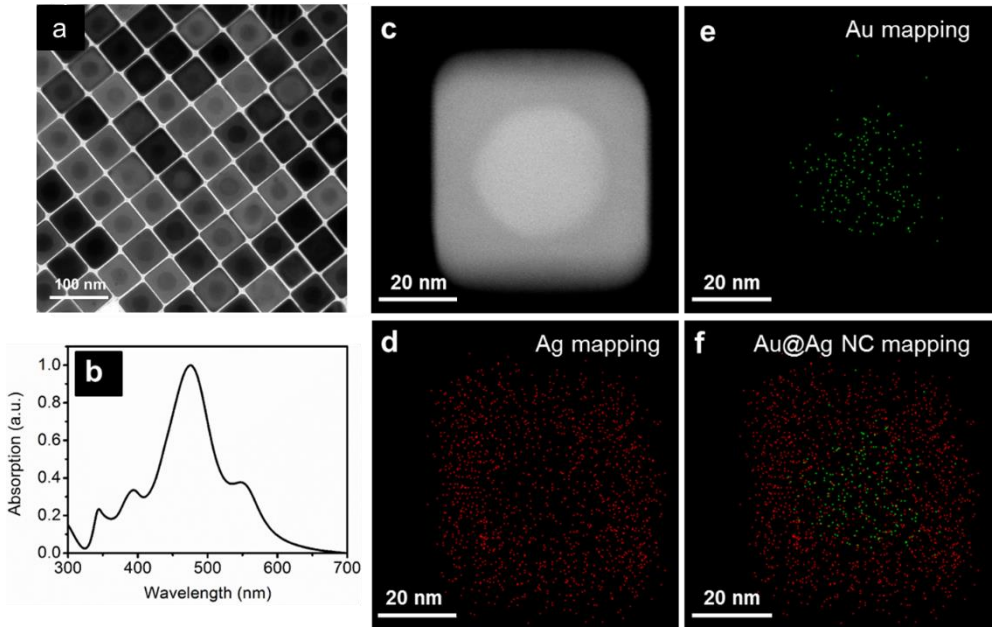

Figure S1. (a) TEM image of Au@Ag NCs with an average diameter of ~55 nm. Scale bar, 100 nm. (b) Normalized UV-vis absorption spectrum for ~55 nm Au@Ag NCs sample in aqueous solution. (c) Typical HAADF-STEM image of a Au@Ag NC. (d-f) Corresponding HAADF-STEM-EDS elemental mapping images of the Au@Ag NC in c. Scale bar, 20 nm.

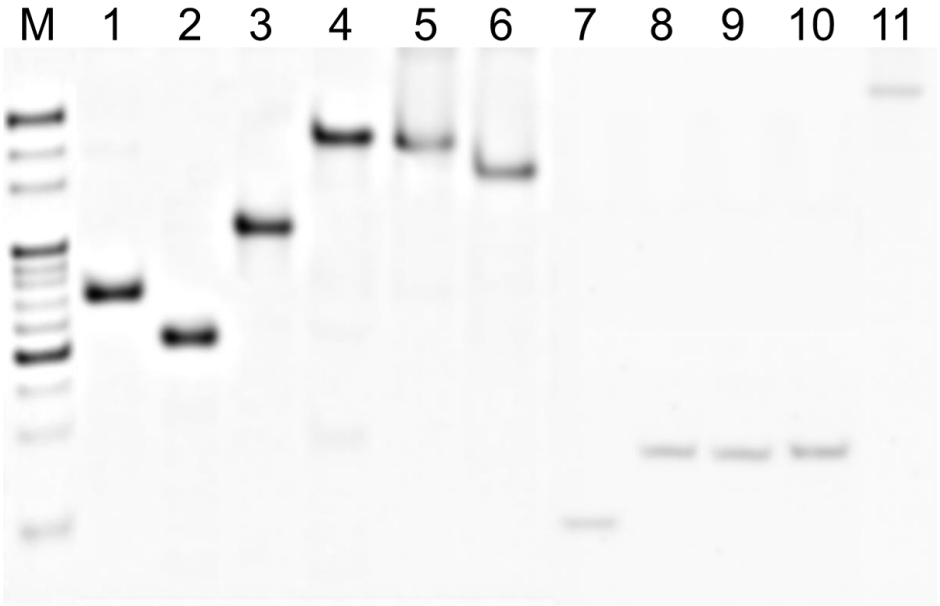

Figure S2. Polyacryamide gel electrophoresis (PAGE) analysis of the formation of the $tsDNA_{17}$. Lane 11 represents a $tsDNA_{17}$. Control experiments for two strands (lane 1, 2) or any other combinations lacking one (lane 3, 4, 5, 6) or single-stranded (ss-) DNA (lane 7, 8, 9, 10). Lane M, 20 bp ladder.

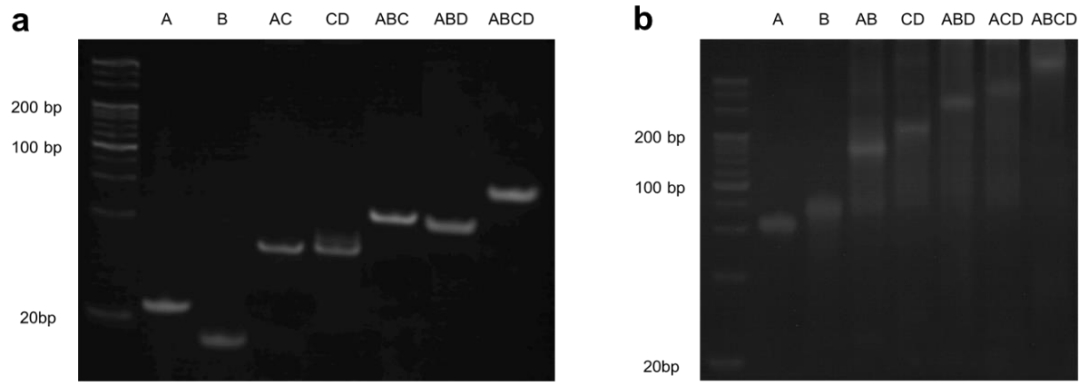

Figure S3. PAGE analysis of the formation of the (a) $tsDNA_7$ and (b) $tsDNA_{26}$.

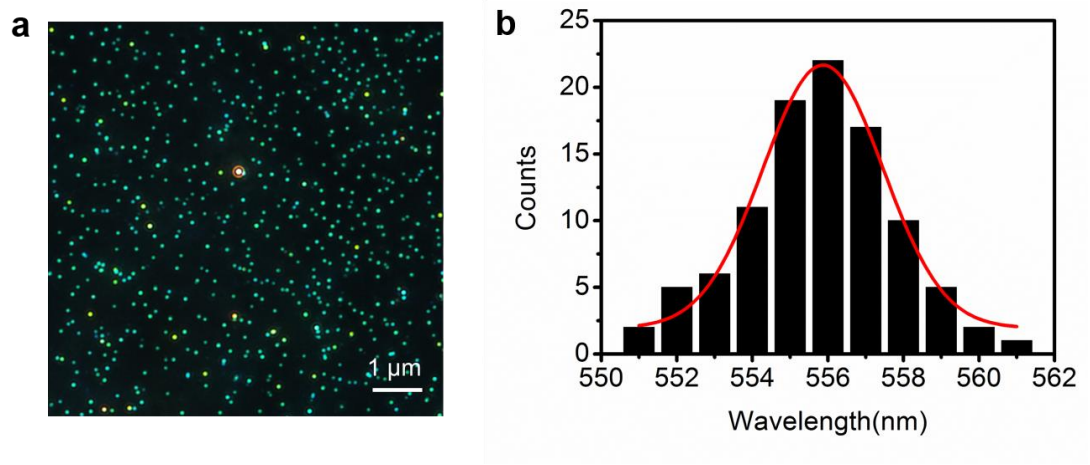

Figure S4. (a) DFM image and (b) calculated wavelength of the Au@Ag NCs-$tsDNA_{17}$ probes.

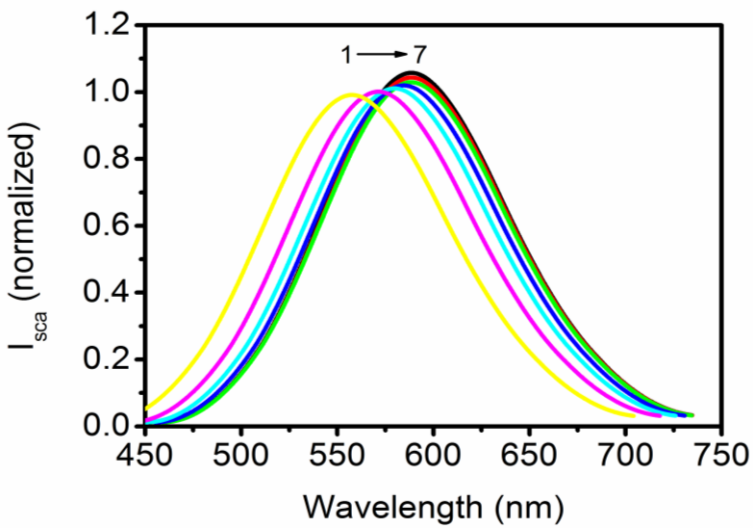

Figure S5. Representative scattering spectra of single Au@Ag NC-tsDNA$_{17}$ probe obtained at different times after adding 1 pM miR-21, showing that the λ_{max} of the LSPR spectrum is redshifted, spectra 1-7: 0, 30, 60, 90, 120, 150, 180 min.

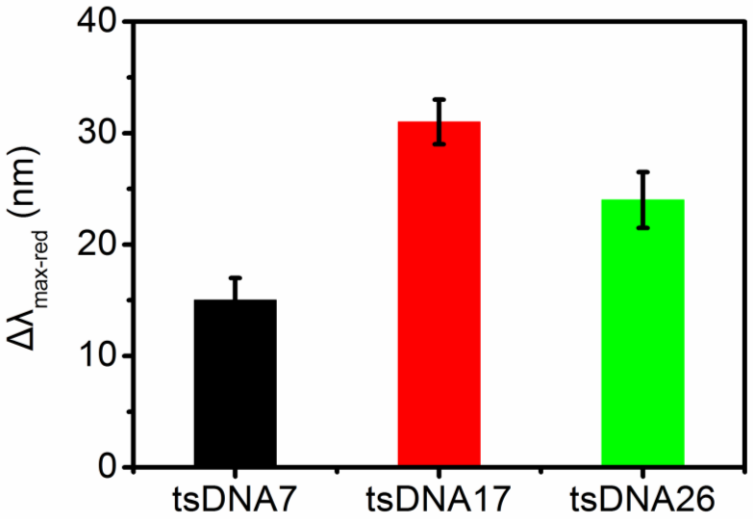

Figure S6. Peak shifts of three types of Au@Ag NC-tsDNA probes under the same reaction conditions. The $\Delta\lambda_{max\text{-}red}$ values were 15, 31, and 24 nm for tsDNA$_7$, tsDNA$_{17}$, and tsDNA$_{26}$, respectively. The final concentration of tsDNA$_7$, tsDNA$_{17}$, tsDNA$_{26}$, and miR-21 in all used solutions is 1 pM.

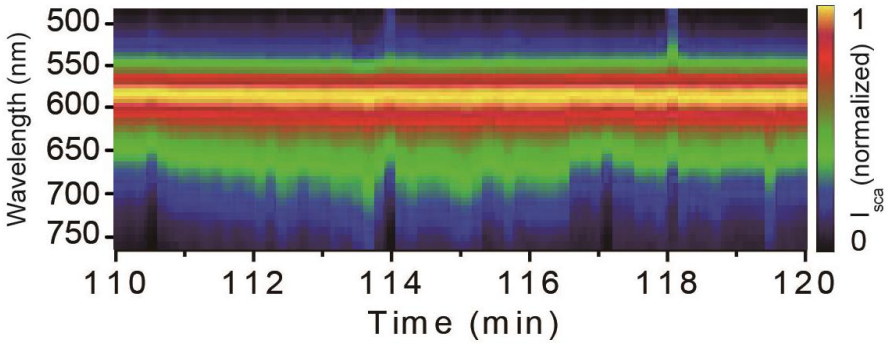

Figure S7. The scattering intensity (I_{sca}) as a function of time when a single Au@Ag NC-tsDNA$_{17}$ probe hybridized with 1 pM of miR-21 during the interval from 110 to 120 min. The final concentration of tsDNA$_{17}$ and miR-21 in the used solutions is 1 pM.

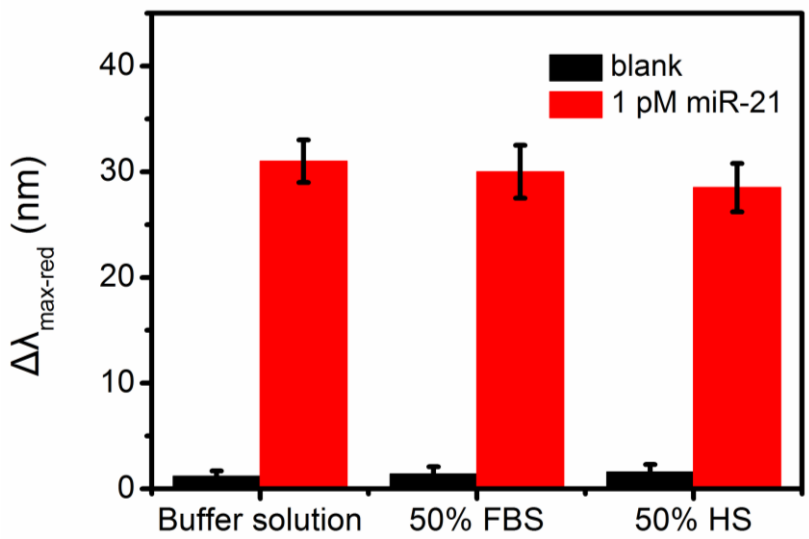

Figure S8. Plasmonic nanobiosensor for miR-21 assay in several media. From left to right: 1 pM miR-21 in buffer solution, 1 pM miR-21 adulterated in 50% fetal bovine serum (FBS), and 50% human serum (HS).

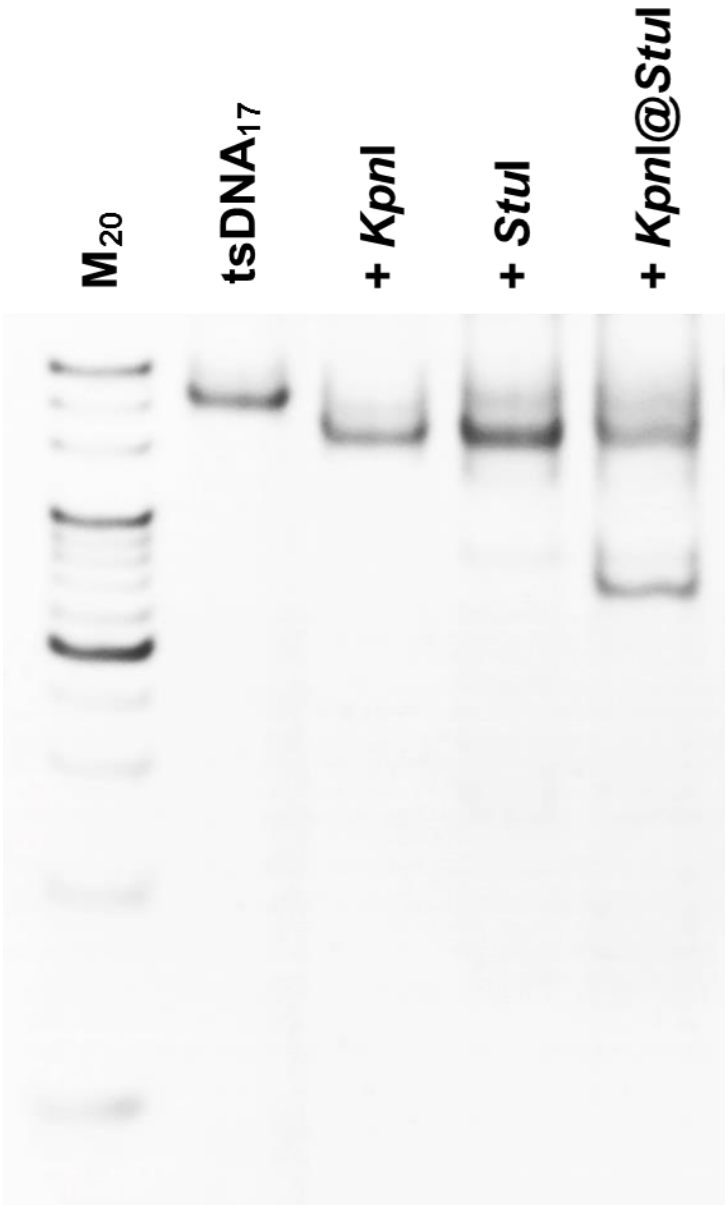

Figure S9. Cleavage of $tsDNA_{17}$ with endonucleases. Test digestion of $tsDNA_{17}$ with endonucleases *Kpn*I and *Stu*I was performed according to the manufacturer's instructions from Takara Biotechnology Co. Ltd. (Dalian, China). The cleavage sites for the two endonucleases are shown in Table S1. For cleavage reaction of $tsDNA_{17}$, 1 µL of each of the endonucleases was mixed with appropriate amounts of buffer and water in 50 µL of final reaction volume. The reaction was incubated at 37 ^{o}C under constant mixing in the shaker for 15 min. The digestion was then verified by 8% PAGE in 1X TBE, with a 20 bp ladder as a molecular weight standard provided from Takara Biotechnology Co. Ltd. (Dalian, China).

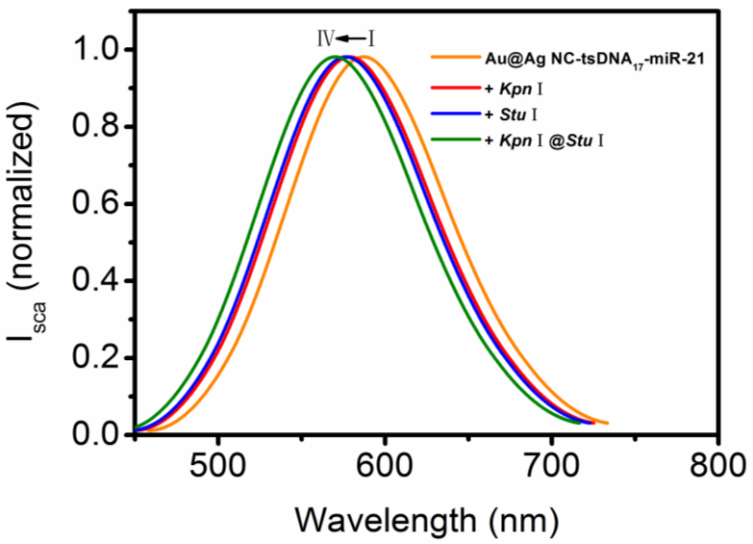

Figure S10. Typical scattering spectra of Au@Ag NC-tsDNA$_{17}$-miR-21 nanoconjugates before (I) and after cleavage by endonucleases *Kpn*I (II), *Stu*I (III) and *Kpn*I@*Stu*I (IV), showing that the λ_{max} of nanoconjugate is blue shifted.

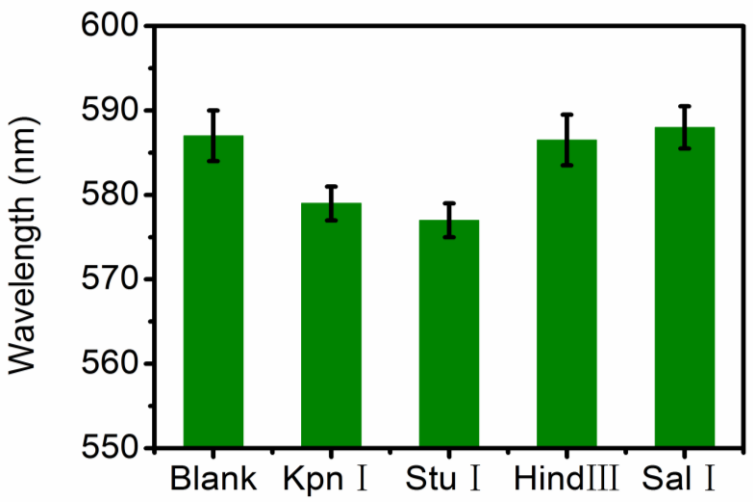

Figure S11. Selectivity tests of the Au@Ag NC-tsDNA$_{17}$ probes, using *Kpn*I, *Stu*I, *Hind*III and *Sal*I with the same concentration. The error bars represent the standard deviation in the measurements of 50 nanoparticles.

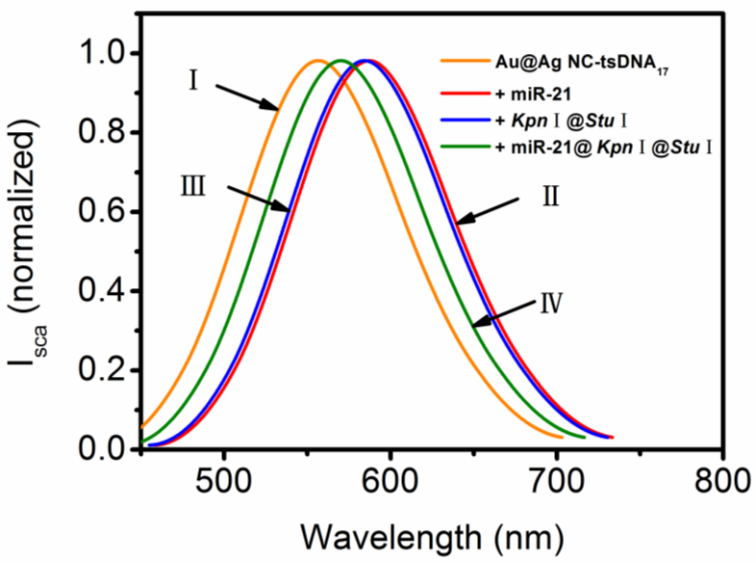

Figure S12. Typical scattering spectra of Au@Ag NC-tsDNA$_{17}$ probes before (I) and after addition of either miR-21 (II) or endonucleases (*Kpn*I and *Stu*I) (III) as well as both miR-21 and endonucleases (IV), showing the shift of λ_{max} of Au@Ag NC.

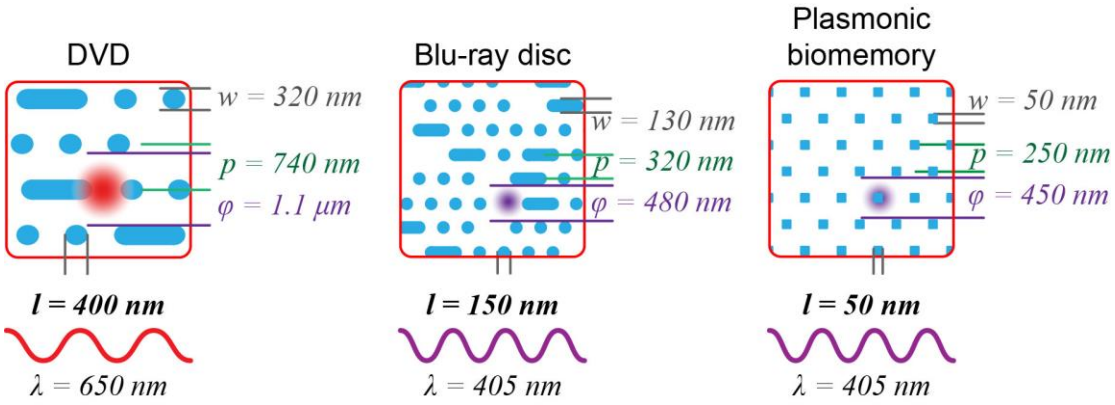

Figure S13. Comparison of various characteristics of a DVD, Blu-ray disc and plasmonic biomemory. (track pitch *p*, pit width *w*, minimum pit length *l*, laser spot size φ and laser wavelength λ)

References

(1) Ma, Y.; Li, W.; Cho, E.; Li, Z.; Yu, T.; Zeng, J.; Xie, Z.; Xia, Y. *ACS Nano* **2010,** *4*, 6725-6734.
(2) Pei, H.; Lu, N.; Wen, Y.; Song, S.; Liu, Y.; Yan, H.; Fan, C. *Adv. Mater.* **2010,** *22*, 4754-4758.
(3) Hu, Y.; Zhang, L.; Zhang, Y.; Wang, B.; Wang, Y.; Fan, Q.; Huang, W.; Wang, L. *ACS Appl. Mater. Inter.* **2015,** *7*, 2459-2466.
(4) Palik, E.D. *Academic Press.* **1985.**
(5) Harrington, R. E.; *J. Am. Chem. Soc.* **1970,** *92*, 6957-6964.
(6) Chen, J.; Zhou, G.; Chang, C.; Lee, A.; Chang, F. *Adv. Mater. Interfaces.* **2014,** *1*, 1300074.